

Comparing Between Effect of Plasma and Heat Treatment and on Wear behavior of Ni-B-CNT Electroless Coating on AISI 4340

Alaa Mohammed Hussein Wais¹, Abdul Raheem K. Abid Ali², Farzad Mahoubi³

¹Al-Mustaqbal University College, Iraq

²University of Babylon, Iraq

³Amirkabir University of Technology, Iran

Article Info

Volume 83

Page Number: 7199 - 7221

Publication Issue:

March - April 2020

Abstract

The aims of the work are to study the hardness, resistance of wear of plus plasma-nitriding and heat treatment of coatings with electroless Ni-B-CNT. Various concentration of CNT range, 0 g/L, 0.35 g/L and 0.7 g/L in (Ni-B-CNT) composite is deposited on 4340 steel in electroless immersion. Following the procedure of plating, every sample was plasma-nitriding in atmosphere consist of 50% N₂-50% H₂ at (400°C) for (4h) were compared with those of annealed one. The wear behavior and friction of a composite that plating were valued by pin on disk technique used load applied of (10N). The electroless Ni-B-CNT coatings are prepared by using nickel chloride as source for nickel in alkaline bath, borohydride act as reducing agent and used Multi walled carbon nanotubes (MWCNT). The formulas are characterized with FESEM, microhardness, XRD and surface roughness measurements. Surfaces of worn areas were studied with EDS spectroscopy and FESEM. Results of that microhardness are show that the larger hardness of 1250 HV is obtained for (Ni-B 0.35g/L CNT) plasma-nitriding formula whereas the greatest hardness of 1010 HV is become for sample of (Ni-B 0.35g/L CNT) heat treated. As a results, enhance the concentration of CNTs caused structure of coated Ni-B conversion from amorphous to crystalline. The present of CNT not just decrement the size of grain to plasma-nitriding and heat treated formulas but also prevent extreme heat production through procedure of test wear and the friction coefficient is decreased through that test. Furthermore, image of surface worn of Ni-B 0.35g/L CNT plasma-nitriding sample detect the smoothest wear trace the highest wear resistance and not apparent cracks among all the samples was achieved. whilst, in formula of Ni-B-0.7g/L CNT, and agglomeration that occur create roughness in addition to big particles with weakly joined in matrix of Ni in ultimately led to increase in the wear rate.

Keywords: Electroless Ni-B-CNT coating; Plasma-nitriding; Heat treatment; Microhardness; resistance of wear

Article History

Article Received: 24 July 2019

Revised: 12 September 2019

Accepted: 15 February 2020

Publication: 06 April 2020

1. Introduction

In recent times, plating technique by using of aqueous solutions (electroplating plus electroless plating) obtain a great consideration due to the aims such as easy of the coating technique, high deposition rate, low cost, preparation of uniform layer of coating plus promising final properties like good wear resistance, high hardness, and a good anticorrosion properties [1-4]. Electroless nickel coating technique is more famous as compare with aqueous solution metal deposition technique, also has experienced notable modifications so its discovery by Branner and Riddell in 1946. The technique has some distinct features like uniform high hardness, thickness, abrasion resistance and good wear, good solderability, excellent corrosion resistance, amorphous and/or microcrystalline deposit, high reflectivity, low friction coefficient, low resistivity and good magnetic properties. Their work led to the development of the 'kanigen' process (catalytic nickel generation) by the General American Transportation Corp (G.A.T.C.) which launched a pilot line in 1955 [5]. The first borohydride reduced bath was proposed in 1954 and the technology was developed in 1957-1958, less than 20 years after the first synthesis of sodium borohydride [6]. Applications of electroless coatings are used in different areas such as powder metallurgy, MEMS, electromagnetic interference (EMI), heat exchangers, reactor membranes, and reduction of bacterial adhesion. Electroless coating technique has the advantage of thickness uniformity when compared with the electrodeposition technique [7-10]. The apparent advantage of boron and promising benefit of electroless coating technique, enhance properties of surface by depositing Ni-B coating during electroless coating technique be concerning as a reasonable choice. Following its maturity, repeatability and scalability in 1989, Ni-B

electroless coating technique was adopted as a mass production technique. The electroless Ni-B coating technique is obtaining remarkable attention to enhance the properties of surface of a large variety of substrates [11-12]. Electroless (Ni-B) coating formation a uniform coatings that contain significant amount of nickel boride that induces substantial enhancement in wear plus abrasion properties [13-15]. Different type of substrate materials can be used including stainless steels, carbon steels, aluminium plus aluminium alloys, iron, glasses, plastics. The advantage of electroless Ni-B coatings involve a good hardness (higher than tool steels), extreme wear resistance (superior as compared with hard chromium coatings) plus promising corrosion resistant features (Ni-P coatings). In addition to these advantages, uniform thickness, low cost, good lubricity, high wear resistance, corrosion resistance and promising ductility, marvelous solderability, high electrical properties, high bonding, good conductivity [16]. commonly, electroless Ni-B coating technique is thought to be better when compared to Ni-P plating also more attractive in many industries [17,18]. Little of investigators have worked Ni-B heat treatment of Ni-B in a vacuum with nitriding plasma [19]. Improved mechanical properties, resistance of wear and resistance of corrosion, and nanocomposite coatings have great deal of attention. Nanocomposite coating has another appropriate identified solid lubricants like MoS₂ [20], PTFE [21] and CNT [22] in which can act to decrement the friction coefficient with enhance the resistance of wear on surface. Because of great tensile strength of carbon nanotubes with elastic modulus [23], make it widely used in ceramic composites and metallic composites such Cu-CNT [24], ZrO₂-CNT [25] and Ni-P-CNT [26]. Plasma nitriding

can be executed with equal temperature ranged for heat treatment of Ni-B-CNT coatings and a good treatment for enhancing properties of the surface for different engineering materials, it can be used for post-treatment of electroless Ni-B-CNT coatings [27].

The aim of this studying is explain effects behaviour of electroless Ni-B-CNT coating with various concentrations of CNT, Plasma nitriding and heat treatment coating on mechanical properties (microhardness and wear

resistance), and microstructure of 4340 alloy.

2. Experimental

2.1. preparation of Substrate

The substrate metal used in this work was AISI 4340 steel grade . specimens (20mm diameter×10mm height) were used as the substrates. The chemical analysis for this alloy and details composition (weight %) is shown an Table (1).

Table (1): chemical Compositions of 4340 steel

Element	C	Si	S	Mn	P	Cr	Ni	Mo	Fe
AISI	0.3-0.45	0.2-0.4	Max 0.04	0.5-0.8	Max 0.04	0.6-0.9	1.25-1.75	0.15-0.25	Bal .
W%	0.36	0.29	0.01	0.67	0.01	0.81	1.3	0.15	Bal .

To enhance the mechanical properties like toughness and hardness, the base metal were undergo to heat treatment (hardening and tempering), heating at 850°C for one hour then quenching in oil. Following, the substrate is tempered at in temperature 400°C for one hour, then cooling in furnace to room temperature. .All specimens are grinded and polished as ASTM by emery paper (tungsten oxide paper) No.(180-2000) respectively. Then samples were washed by distilled water and ethanol, and dried by using an electrical dryer. A polishing is conducted by diamond paste , specimens were immersion in acetone for 30 min, Before coating ,Specimens are immersion in solution electro cleaning include materials

(60g/l NaOH ,38g/l NaCO₃ and 30g/l NaPbO₄) for one minutes period at 70°C temperature with moving the electrolyte using magnetic stirring with(5 volt)in order to eliminate the dust and the oil from the metal surface, follow that specimens are wash by distilled water, The specimens dry with using dryer of an electrical and after that ,it directed immersion in coating solution and Immersion of specimens in electroless Ni-B bath immediately.

2.2. CNT ball-milling

MWCNT with purity more than 95%, 10-30 µm with length,5-10nm in inside diameter and 20-30 nm in outside

diameter, are bought from (US Nano materials Research). For to enhance dispersion for CNT in electroless coating bath, as-received CNT were ball milled at (3 hours) using by machine of planetary ball-mill with balls of steel with various diameters have been used for mix CNT in cylindrical stainless steel jar, rotating speed and then (10 min) fracture intermitting each (20 min) of milling to reduce heat build-up. In wet mixing used Ethyl alcohol. Figure(1) shows Field Emission Scanning Electron Microscopy in MIRA3 TESCAN company in Iran, images of ball milled and as-received CNT. The image show to ball milled CNT are smaller and the most straight so to enhance dispersion for CNT at bath of electroless. For dispersed uniformly CNT in Ni-B electroless coatings and prevent agglomeration to provide stable and homogenous dispersion in the metallic matrix phase. Should use surfactants SDS (sodium dodecyl sulfate) with CNT and together mixed with water by ultrasonic device for 45 min.

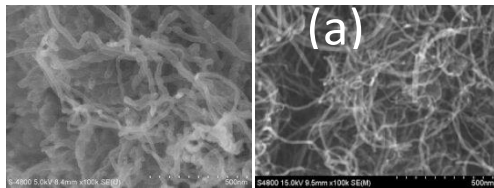


Fig.1. FESEM images of (a) as-received CNT and (b) ball milled CNT.

2.3. Electroless bath preparation

After completion of preparing surfaces for coating, electroless bath were prepared for the process according to concentrations shown in Table (2). The coating of Ni-B was deposited on the 4340 steel via electroless coating procedure. pH value of coating bath was varied between (12-14). The coating of Ni-B was deposited on the 4340 steel via electroless coating procedure. pH value of coating bath was varied between (12-14). The coating electroless of Ni-B perform at $(95 \pm 1^\circ\text{C})$ for (60 min). Through of coating, solution of bath agitate by a magnetic stir to avoid localized overheating and reduce the fluctuation of ionic concentration. Every 10 min the sample was revolved about two opposite directions to get constant plating thickness. As the coating procedure of Ni-B-CNT deposition by various concentration of CNT (0.35g/L, 0.7g/L CNT), firstly CNT were dispersed in ultrasonic bath, then addition of CNT to the Ni-B prepared bath. Figure(2) shows the setup of electroless composite deposition. After the completion of the process of coating, specimens were placed inside a vacuum oven, to dry for 30 minutes, at a temperature 50°C .

Table (2): Operating conditions for electroless bath.

Bath composition	g/L
Nickel chloride ($\text{NiCl}_2 \cdot 6\text{H}_2\text{O}$)	24

Sodium borohydride (NaBH ₄)	0.8
Ethylenediamine (98%) (EDA)	60 ML/L
Lead Nitrate	0.02
Sodium hydroxide (NaOH)	90
Sodium Dodecyl Sulfate (SDS)	2
Carbon nanotube(CNT)	0, 0.35, 0.7
Operating conditions	
pH	(12-14) OR 13
Temperature	95 °C
Time	1 HR

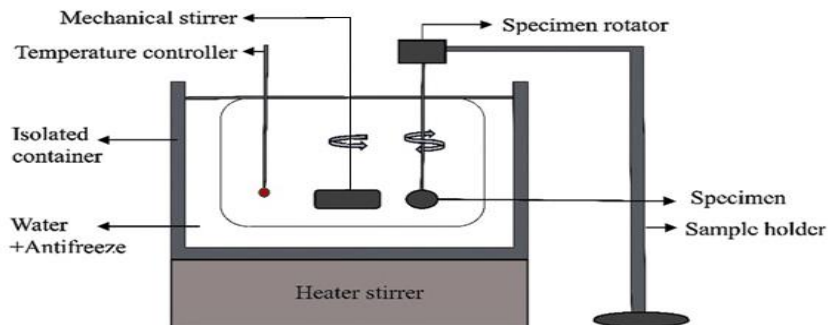


Fig.2. Setup of experimental for electroless deposition.

2.4. Plasma nitriding and heat treatment of coated samples .

After the deposition, every samples (Ni-B, Ni-B-0.35g/L CNT, Ni-B-0.7g/L CNT) degreased acetone follow that are placed in a 5kW direct current of plasma

to increase PECVD (chemical vapor deposition) chamber. annealing process was conducted in vacuum furnace for electroless coating samples at 400 °C for 4 hour. working conditions for the nitriding treatments for electroless bath, is shown in Table (3)

Table (3): Operating conditions of plasma nitriding treatment.

conditions	Pluse Dc plasma nitriding (PPN)
Temperature (°C)	400 °C
Pressure	10 ⁻³ torr
discharge voltage	400-500 V
Frequency	8.9 kHz
Duty cycle	70%
Current(A)	2-3
Gas composition	(50%N ₂ -50%H ₂)
Duration (h)	4

2.5. Characterization

Microhardness of the coating layers were measured by using (TH-717 Vickers hardness tester), 25 g load was applied for 15 sec. Three readings were recorded for each specimen coated and one at the substrate. Then, the average value was taken. Test of Wear is performed about room temperature (25°C) and relative humidity of at (40%). The used load was 10N. Velocity of sliding is (0.1 m/s) and distance of sliding is (500m). The disc was carbide steel. The specimens are weighed by a sensitive scale before and after the wear test to calculate the mass loss of coatings. The specific wear rate of the specimen is calculated (ASTM G99) using ($W_s = \Delta w / \rho F S$), any (W_s) is specific wear rate, (Δw) is weight lost of specimen, (ρ) is the density, (F) is normal load (N) and (S) is distance of the sliding (m).

The value of roughness of surface measurement is carried out to the coated

samples before and after the heat treatment and treatment of plasma nitriding using a common parameter Ra in μm . In test of surface roughness calculate a mean of (10) measurements was recorded.

Examined of coatings to crystalline phase identification. identification of coating phase is by (EQuinox X-3000, by Cu Ka(X=1.54187Å) radiation and scanning domain of 20 between (5° and 118°, worked on (40kV and 30mA)) is used, to identification to samples crystal structure before and after heat treatment and the treatment of plasma nitriding.

3. Result and discussion

3.1 XRD

Patterns of XRD of coating Ni-B shows are presented in Figure(3). A broad peak XRD pattern of deposited electroless Ni-B coating was shown in Figure(3) in which indicates that an amorphous

structure. This result was also have been reported by manypapers have stated an amorphous for coating Ni-B. Amorphous element as boron avoids the nucleation of nickel phase [28]. Peak broadening is noted reduce when addition CNT in the electroless bath, and as increase the concentration of CNTs in the electroless bath the peak became sharper, and this can be determined with the effects in samples of (Ni-B-CNT) when ions H^+ are liberate from sets carboxylic that present about the surface of CNTs while residual ions ($HCOO^-$) work as reducing agent ,so, decreases the ions Ni . consequently, begin Ni in the nucleation at flaws of the crystal for CNT in that work a site of nucleation and the microstructure of coating Ni-B-CNT became more semi-crystalline with increase CNT concentration. The same phenomena can been observed with addition SiC particles

[29]. The microstructure of coated specimens is altered from amorphous to crystalline state follow the plasma nitriding treatment in Figure(4),because formation of intermetallic compounds Ni_2B and Ni_3B . They can be appealed the present of the Ni_3B phase is product from the decomposition of unbalanced(Ni_2B) phase or too may be the product for the a distribution irregular of boron by a concentration small. In addition to that, constant the bombardment of a state cathodic by ions of positively charged can be in increment at temperature of surface of specimens then led for growth of Ni_2B and Ni_3B phase. The peak that noted at every specimens may be related to microstructure of boron nitride (BN) [30]. The sputtered boron atoms in plasma atmosphere reacted with active nitrogen and form BN after that deposited on the specimen surface.

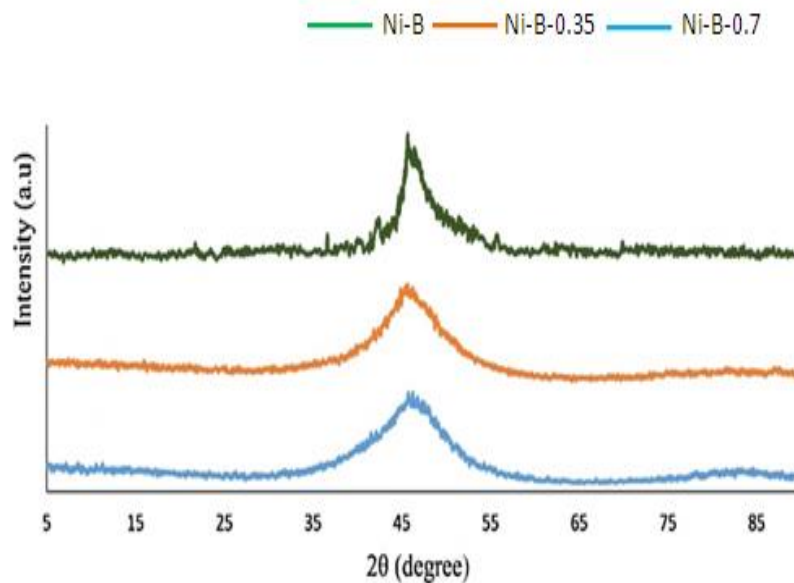


Fig.3. Patterns XRD for plated samples(Nickel-Boron and Nickel-Boron-Carbon nanotube).

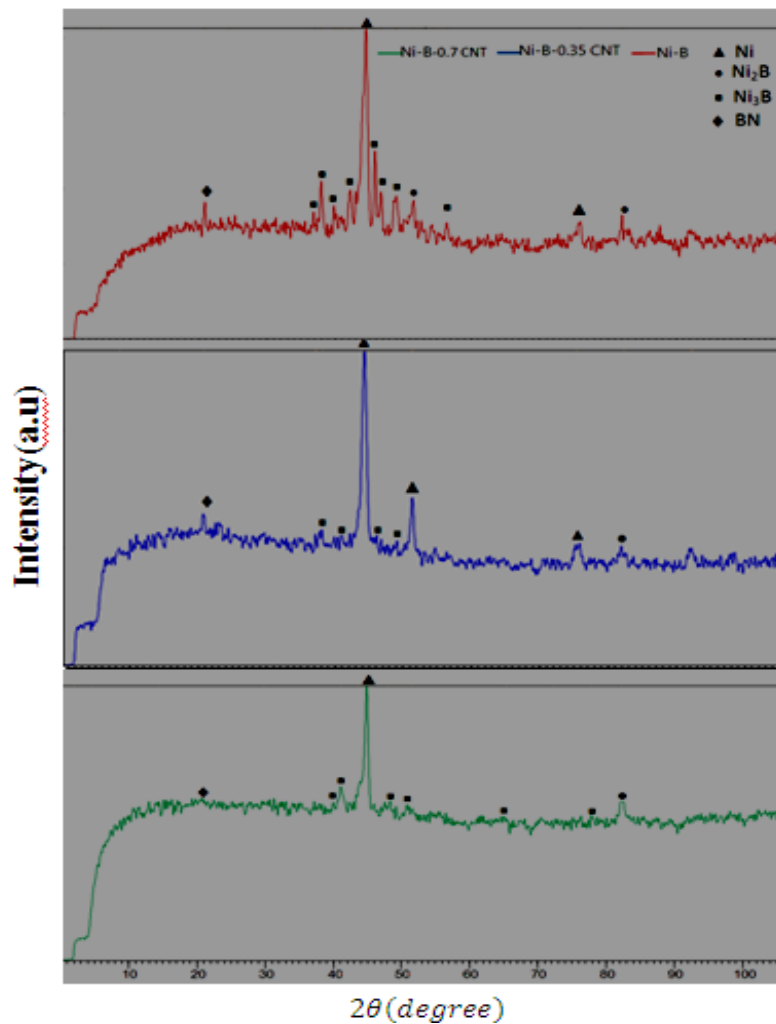


Fig.4. Patterns XRD for plasma nitriding samples(Nickel-Boron and Nickel-Boron-Carbon nanotube).

3.2 Surface Morphology.

Figure(5) show morphology of surface of the coated sample, in which the smooth microstructure of Ni-B sample can be noted in image in Figure(5a) and exhibit a cauliflower type microstructure. These type of structure can be benefit in keeping lubricants below conditions of adhesive wear [31,32]. A larger part of the CNT are found fixed in the matrix through the particle distribution while the lesser part are protruded from the surface of coated;

on the other hand, CNTs are present at the surface of specimen containing 0.35g/L CNT in Figure(5b). Furthermore, important change in the microstructure is observed in the specimen containing 0.35g/L of CNT, which seems logical and lead to increase uniformly coated surface, in which CNT have the capability to fill the crevices and gaps because of small concentration for nanotubes. When with increasing concentration at(0.7g/l) of CNT the size large of the growth of nodules. These result related by increased

concentration for reduce Ni at the electroless bath may be could lead in the growth of to nucleation minimize in Figure(5c). The CNTs aggregation that is be observed result from presence of big particles about Ni-B-0.7g/l CNT specimen owing to the great concentration of them. These led to agglomeration of CNT on the

base metal and so consequently big particles on the surface of samples might be shaped related to the nucleation of Ni on agglomeration of CNT. so as to prove the CNT distribution become very clearly, the image by magnification larger for specimen is found in Figure (5d).

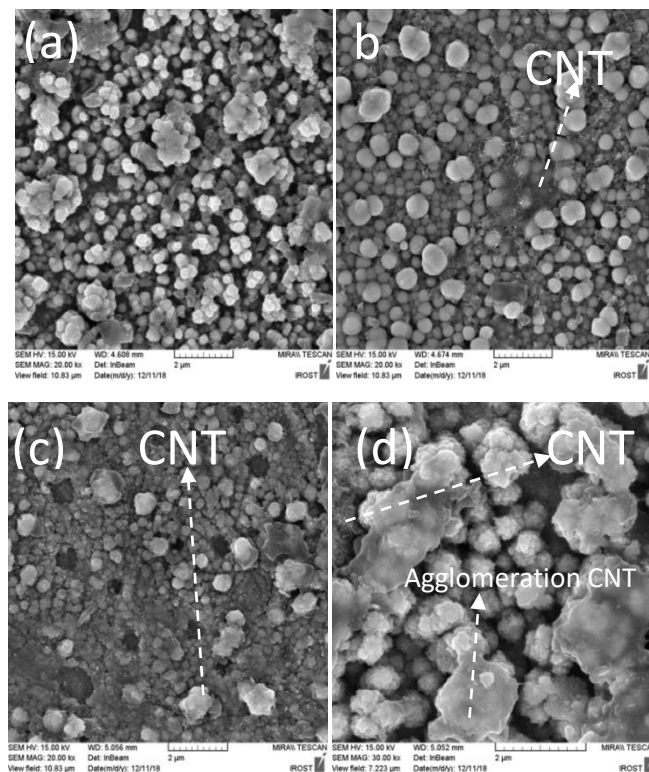


Fig.5. Images FESEM of coated electroless (a) Nickel-Boron, (b) Nickel-Boron -0.35g/l Carbon nanotube, (c) Nickel-Boron -0.7g/l Carbon nanotube, (d) higher magnification of (Nickel-Boron -0.7g/l Carbon nanotube).

Figure(6) FESEM observations of the samples with heat treated show that the coated Ni-B appear semi-bright, while the heat treated of Ni-B coatings are matte in appearance, earlier study is shown which the nodules of Ni-B are nearly flat and uniformly dispersed as-deposited condition, while heat treated a growth of the nodules in size cause to a coarse-grained structure [33].

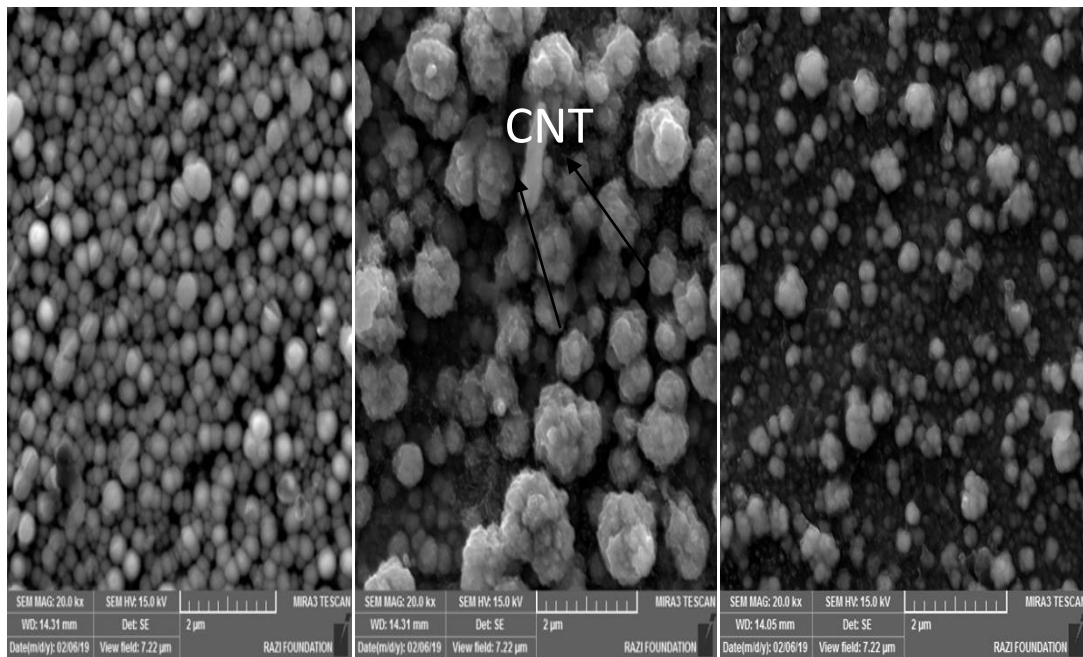


Fig.6. Images FESEM for heat treatment (a) Nickel-Boron, (b) Nickel-Boron-0.35g/l Carbon nanotube, (c) Nickel-Boron-0.7g/l Carbon nanotube

In Figure(7) observations of FESEM for the samples of plasma-nitrided showed change the morphology of surface Ni-B to cauliflower-like microstructure with very clearly in Figure(7a). The type of the structure seen may be due to a perfect deposition in the surface defect sites in begin of process [31,34]. Figure(7b) shown a sample that containing (0.35g/L CNT) same densification is happened. the actuality, growth of the crystals are nucleated initially at diverse favored places has cause Ni_2B , Ni_3B , and BN particles at coincide by cover the surface of the specimen. In addition to that, re-deposition and sputtering of the atoms may worked

the redeposited compounds to fill the spaces through treatment of plasma nitriding. The sample that contain (0.7g/l CNT) had a coarser particles in Figure(7c). Follow the plasma nitriding treatment the agglomerated particles noted to be 2 or 3 times larger and this due to a high CNTs concentration which can causes more rate of growth and nucleation of the nanoclusters in this sample. On the other hand, no indication of the CNTs in the specimen surface of is noted. this final result related, a fixed ion bombardment through process of plasma nitriding has eliminate the too much CNT from the surface.

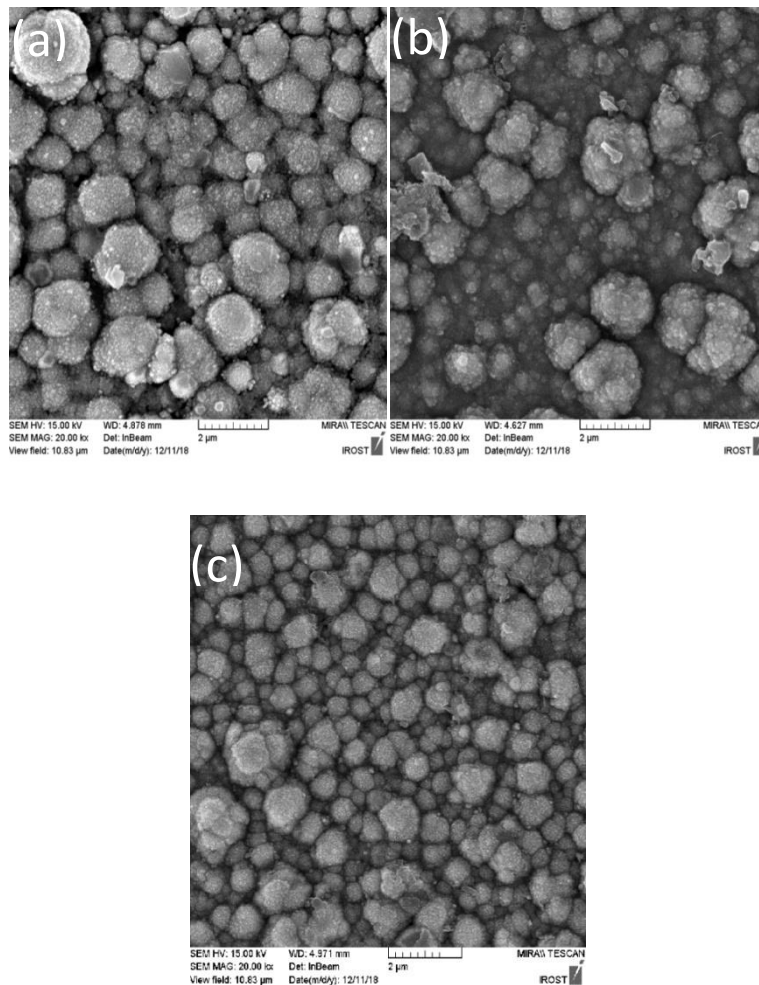


Fig.7. Images FESEM for plasma nitriding(a) Nickel-Boron, (b) Nickel-Boron-0.35g/l Carbon nanotube, (c) Nickel-Boron-0.7g/l Carbon nanotube.

3.3. Surface roughness

Roughness of the substrate data is illustrated in table(4), for-plated, annealing and plasma-nitriding of samples. as-plated, annealed plus plasma-nitrided samples. As mentions above increase CNTs concentration to 0.7g/L cause a significant raising in the roughness. In which CNT prevent uniform growth of Ni plus create of roughness. The sample roughness of Ni-B-0.7g/l CNT is higher when comparison with other specimens, because large concentration of CNT which

may product agglomeration. Plasma-nitrided increased to roughness of the surface (Ra) of the coatings . As redeposition and sputtering are occur through process of CPN , CPN of coating is surface roughness more than the annealing . By plasma nitriding leading An increase in the surface roughness this fact is agreed with [35, 36] .There are three probable explanations for this product. First, follow to the process of Plasma-nitrided, growth of the crystal of BN and Ni₂B, Ni₃B phases at the Ni

matrix create of roughness and source the increased surface roughness .Second, the influence of sputtering through the procedure of Plasma-nitrided, affected with hydrogen of the positive and

bombardment of nitrogen ion , caused on roughness of samples .Third, these result may be because redeposition of sputtering of material on the surface.

Table(4): Results of roughness of samples surface

Specimen	Ra (μ)
Substrate	0.3
(Nickel-Boron) a plated	0.1
(Nickel-Boron-0.35g/l Carbon nanotube) a plated	0.17
(Nickel-Boron-0.7g/l Carbon nanotube) a plated	0.2
(Nickel-Boron) a annealed	0.26
(Nickel-Boron-0.35g/l Carbon nanotube) a annealed	0.24
(Nickel-Boron-0.7g/l Carbon nanotube) a annealed	0.28
(Nickel-Boron) a plasma-nitriding	0.34
(Nickel-Boron-0.35g/l Carbon nanotube) a plasma-nitriding	0.21
(Nickel-Boron-0.7g/l Carbon nanotube) a plasma-nitriding	0.4

3.4 Microhardness

Figure(8) shows the surface of samples microhardness of heat treatment and the plasma-nitrided. As noted, the CNTs reinforcing ability have force in

enhancing the microhardness of surface, particularly in the sample of(Ni-B-0.35g/l CNT).these can be related with reinforcement and uniform distribution of

carbon nanotubes about these specimen. The hardness of (Ni-B-0.7g/l CNT) is less when comparison with the specimen that having (0.35g/L CNT) due to the large CNTs concentration, in addition to that, segregation that happened at the composite led to a decrease in the composite microhardness of coated layer [37]. Increment in the microhardness by

heat treatment is because a related to the conversion from an amorphous to crystalline structure this fact is agree with [97,98]. Follow the procedure of plasma-nitriding increased in the microhardness value occurred, because a creation of Ni₂B, Ni₃B and BN phases [40].

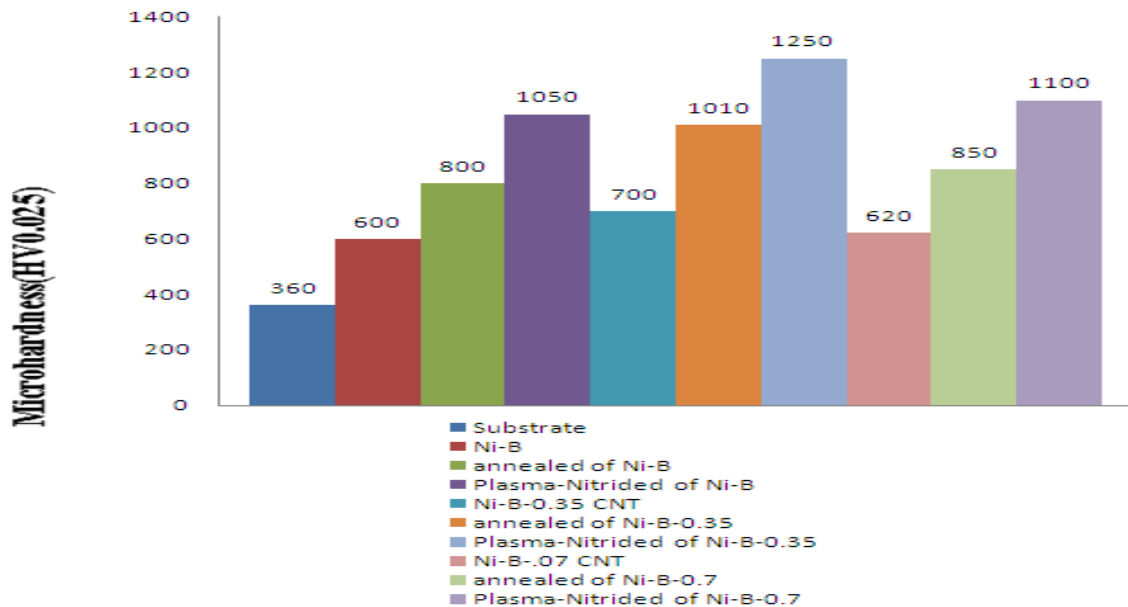


Fig. 8. Microhardness results of as-plated ,annealing and plasma-nitrided of samples surface

3.5. Wear behavior

Figure(9a) express diagram of the friction coefficient for sample of substrate .Figure(9b,c,d) express diagrams of the friction coefficient for samples of as-plated. A substantial variation for coefficient of the friction is showed at sample Ni-B and these related by a large mutual solubility of nickel and iron which can cause in increment in the region of the surface contact coated with counterpart and high elimination for material. A further more explanation for that behavior, and crystallization of an amorphous plated specimen through test of the wear, because of generation of the heat which produce at appearance of stresses of tensile at the

interface of crystalline and amorphous phases. Furthermore during the hydrogen evolution, the cracks is generated on the surface which caused to concentration of stress that enabled delamination through test of the wear and addition increment variation [26,32].

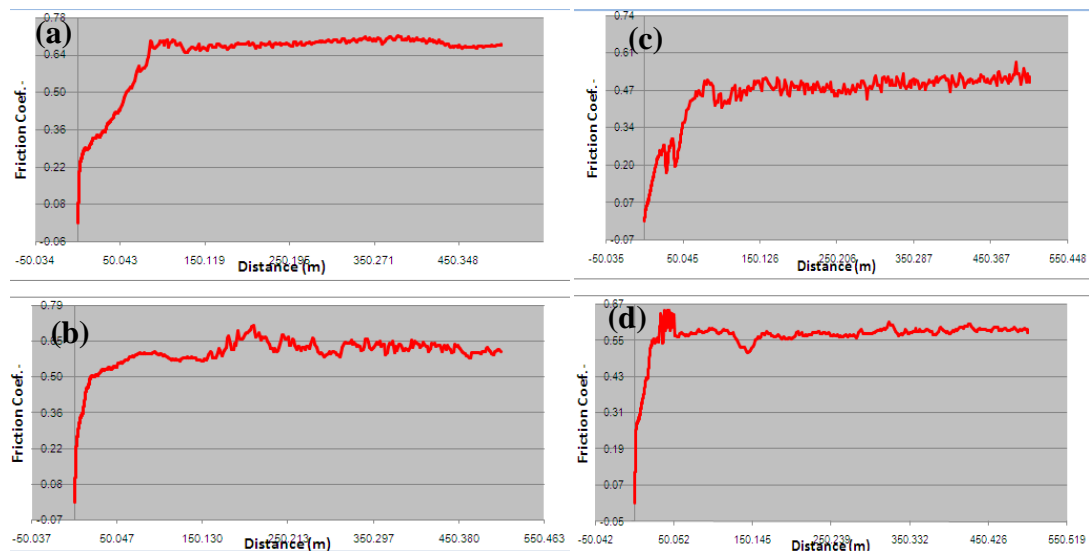
Friction coefficient is decrement with elevate by concentration of CNT to (0.35 g/L) so may be too easy shear of lubricating film of carbon which decrease direct contact among counterpart and surface of samples [41]. Coated specimen of (Ni-B-0.7g/l CNT), the friction coefficient initial increase and subsequently decrease as appeared in Figure(9d). This phenomenon can be

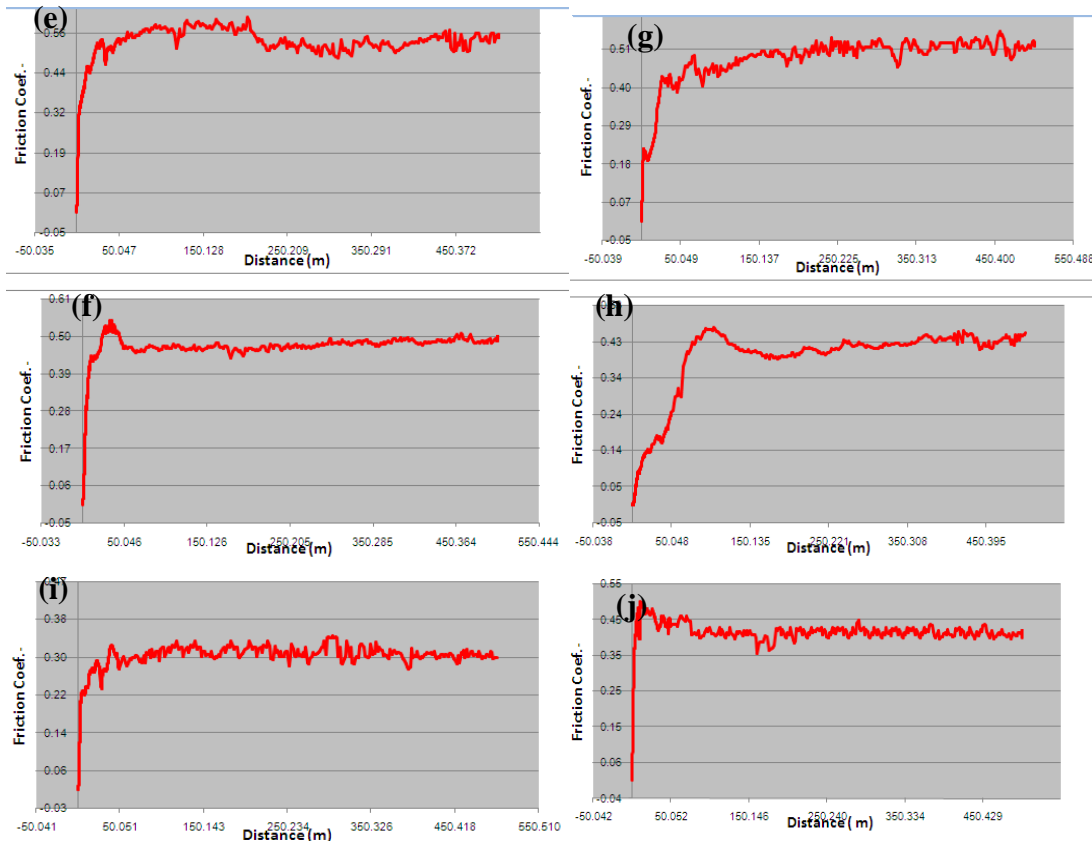
explain by maybe elimination of agglomerated CNT, actually, they not good cohesion with matrix of Ni can cause increment in the specimen wear rate . Follow that due to motion of oxide patches that can produce layer tribo and rolling CNT that effect a separator, decreased coefficient of the friction [42].Additional effects on behavior of wear of samples is roughness of surface. The larger surface roughness can led to interactions of abrasive among the roughness on surface sample of (Ni-B-0.7g/l CNT) and counterpart to be prevailed.

In fact, higher wear rate and friction coefficient result from lesser contact area that cause higher local pressure among the surface and pin of the specimen. Figures(9) illustrate diagrams of the coefficient of friction of plasma nitriding and heat treatment specimen. Follow plasma-nitrided treatment and heat treatment for Ni-B sample, the friction coefficient is clearly decrement. The reasons for this result, high microhardness value that need lower solubility of iron in Ni₂B, Ni₃B and BN particles and more force of friction for plastic deformation. At Ni-B contain CNT

specimens a like decrement direction for coefficient of friction is seen follow treatment of the plasma nitriding .That behavior result from many causes ;firstly the increment microhardness value with the grain refinement. Secondly, through the electroless deposition process, the CNT filled micro-holes of surface which represent the sites of active for stress of tensile. Consequently, CNT can avoid speed of plastic deformation. Thirdly, CNT represented a main barrier to the motion of dislocations. When increment concentration of CNT to (0.35g/l) cause an improvement wear resistance properties and higher reduce in the friction coefficient. In addition ,also CNT can help keep hold of composite hardness at the large temperatures which significant factor because generation of the heat through test of the wear.

In the begin of test period of the wear ,it noted that for plasma nitrided (Ni-B-0.7g/l) and as-plated and also, heat treatment of these samples, increment in friction coefficient. Also, sample of plasma-nitrided follow an about 90 m distance of sliding declined of coefficient of friction in Figure (9j).





Figure(4.9): The friction coefficient differences versus distance (a)substrate sample.(b) Nickel-Boron, (c) Nickel-Boron-0.35g/l Carbon nanotube,(d) Nickel-Boron-0.7g/l Carbon nanotube, electroless coated samples.(e) Nickel-Boron, (f) Nickel-Boron-0.35g/l Carbon nanotube,(g) Nickel-Boron-0.7g/l Carbon nanotube, annealed samples.(h) Nickel-Boron, (i) Nickel-Boron-0.35g/l Carbon nanotube, (j) Nickel-Boron-0.7g/l Carbon nanotube, plasma nitriding samples.

Table (5) illustrated mean of friction coefficient, rate of specific wear and mass loss of as-coated, heat treatment and plasma-nitrided samples. Therefore, it can be noted coefficient of the friction has a relative directly by rate of the specific wear. Also noted the plasma-nitriding (Ni-B-0.35g/l CNT) has the lesser rate of wear specific when contrast to another specimens because of some reasons like

larger microhardness, smaller grain size, lesser coefficient of friction, and mostly of important in homogenous distribution of BN and Ni₂B, Ni₃B particles. wear rate decreases with increasing microhardness and creation of hard phases after the treatments, also the low mutual solubility between those phases and iron could be cause for increasing resistance of the wear[43, 44].

Table(5):Results of average coefficient of friction, mass loss and wear rate of coated samples.

Sample	Coefficient of friction	Specific wear rate (mm ³ /N.m)x 10 ⁻⁴
--------	-------------------------	--

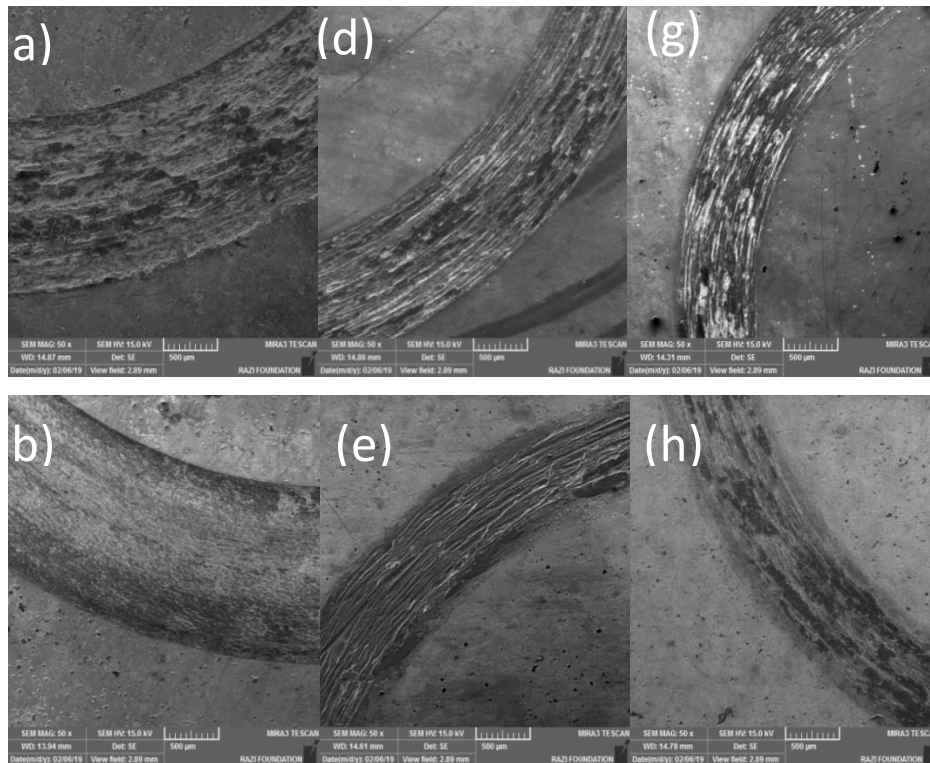
		8
Substrate	0.68	3.4
(Nickel-Boron)a plated	0.61	1
(Nickel-Boron-0.35g/l Carbon nanotube) a plated	0.51	0.9
(Nickel-Boron-0.7g/l Carbon nanotube) a plated	0.59	1.1
(Nickel-Boron) a annealed	0.55	0.9
(Nickel-Boron-0.35g/l Carbon nanotube) a annealed	0.5	0.04
(Nickel-Boron-0.7g/l Carbon nanotube)a annealed	0.53	0.6
(Nickel-Boron) a plasma nitriding	0.45	0.4
(Nickel-Boron-0.35g/l Carbon nanotube) a plasma nitriding	0.31	0.01
(Nickel-Boron-0.7g/l Carbon nanotube) a plasma nitriding	0.41	0.8

Figure(10) explain analysis of FESEM of worn surfaces for samples follow test of wear. Enhancement of wear resistance is clear. Figures(10-11a,b and c)shows deep and wide wear track, sample Ni-B particles of lamellar debris indicated the delamination happen through the test of wear in Figures(10-11a). When CNTs concentration increase to 0.35g/L a fine grooves is noted along the sliding direction, in Figures(10-11 b).According to Figure(12), reduced quantity for iron with contrast by specimen Ni-B is found when analysis of chemical of the remained elements on track of the wear, and this may be because reality that the cut from CNT an action as ball bearing spaced and prevention a connection straight for surface plated and counterpart, so

decrement in element diffusion of iron on the plated surface [45].Consequently, by enhancing the CNTs concentration to 0.35, because of founded the surface of lubricated, so, touch for surface with the counterpart less and increase in wear resistance can be occurred. At(Ni-B-0.7g/l CNT) specimen inFigures(10-11 c), deeper groves could be noticed because of the parting of agglomeration particles in which have weak bonding energy on the surface through test of the wear [46]. After nitriding the wear track became shallower and narrower besides when comparison to the annealed coating and a plated coating , the formation of smooth oxidized pitch and the relative dark with the morphologies of track of the wear indicate the minor abrasion at the wear

procedure and domination of oxidation wear for this sample in addition to oxygen amount in samples of plasma-nitriding of Ni-B-CNT is less when contrast with sample Ni-B and these result is approved by EDS. These result attributed to the reality this CNT could avoid generation of the excessive of heat through test of the wear; hence, plastic deformation is declined and observed a lower debris and smooth surface plus grooves fine in the FESEM image (Figures(10-11e)). Nitrided coating has smaller and less sharp debris as well as higher surface hardness and more gentle hardness profiles in comparison to the annealed coating wear debris of annealed coating (highly effort hardened) wedged among the loaded surfaces and motivated along with the pin, resulting the feature parallel abrasive grooves on annealed coatings [53]. The

uniform distribution of particles with higher microhardness values in the matrix of Ni which assist transfer of force of the counterpart from (Ni) to the (CNT)in which produce in larger for resistance for wear at the plasma -nitriding of specimen(Ni-B-0.35g/l CNT) [45]. In addition to that, lower size of grain when the comparison with the other samples of plasma nitriding, its additional cause why Ni-B-0.35g/l CNT possessed the smoothest of wear trace (Figures(10-11e)). Study of the sample of (Ni-B-0.7g/l CNT), detected the to found of fine debris follow test of the wear in which attributed in the particles coarse that the cut from surface because of the pin incessantly motion on the surface (Figures(10-11f)). The motion of particles remained some scratch at surface of sample which decrease of wear properties.



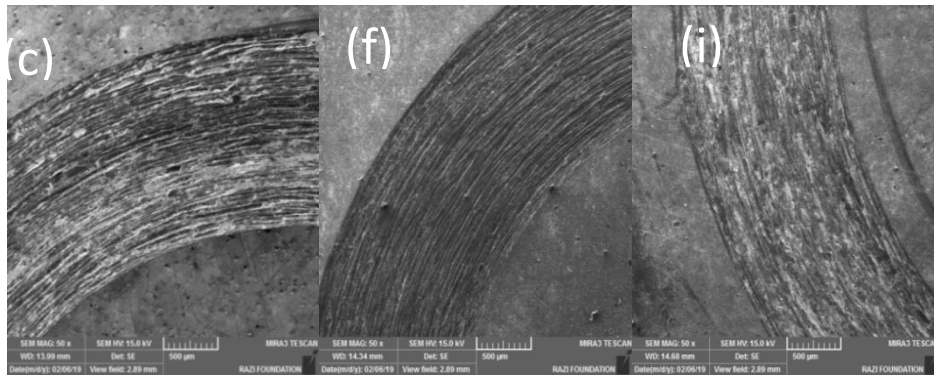
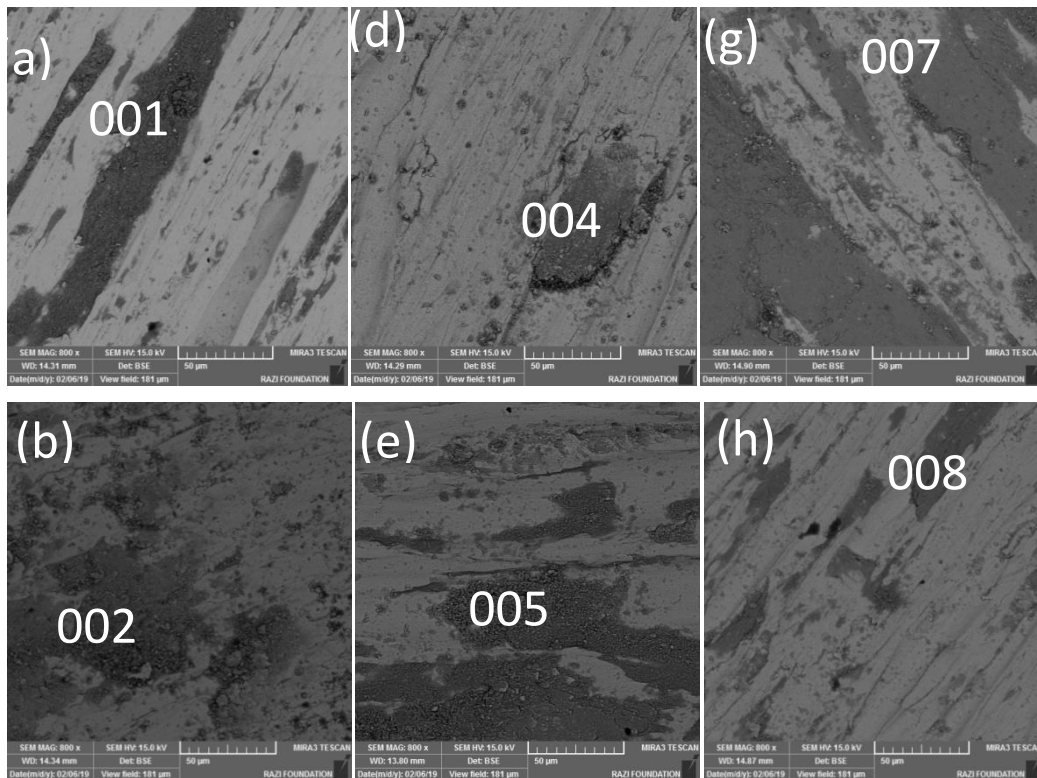


Fig.10. FESEM micrographs of wear track the of (a) Nickel-Boron, (b) Nickel-Boron-0.35g/l Carbon nanotube, (c) Nickel-Boron-0.7g/l Carbon nanotube, as-plated; (d) Nickel-Boron, (e) Nickel-Boron-0.35g/l Carbon nanotube, (f) Nickel-Boron-0.7g/l Carbon nanotube as-annealed; (f) Nickel-Boron, (g) Nickel-Boron-0.35g/l Carbon nanotube, (i) Nickel-Boron-0.7g/l Carbon nanotube,plasma nitriding samples.



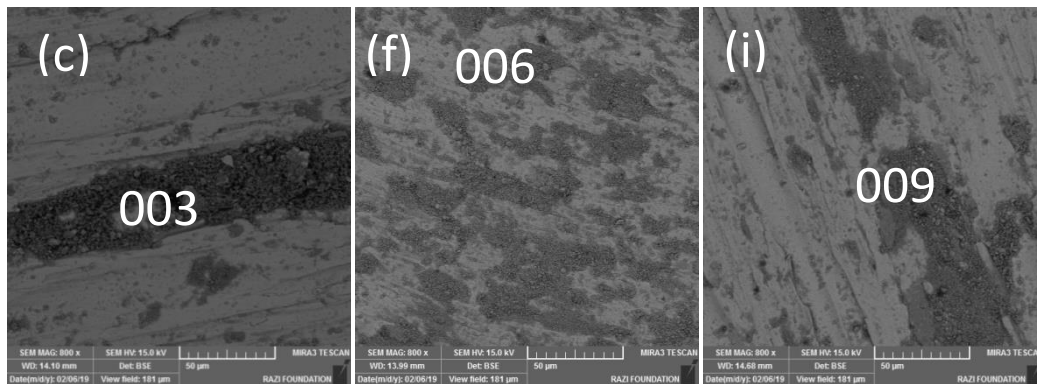
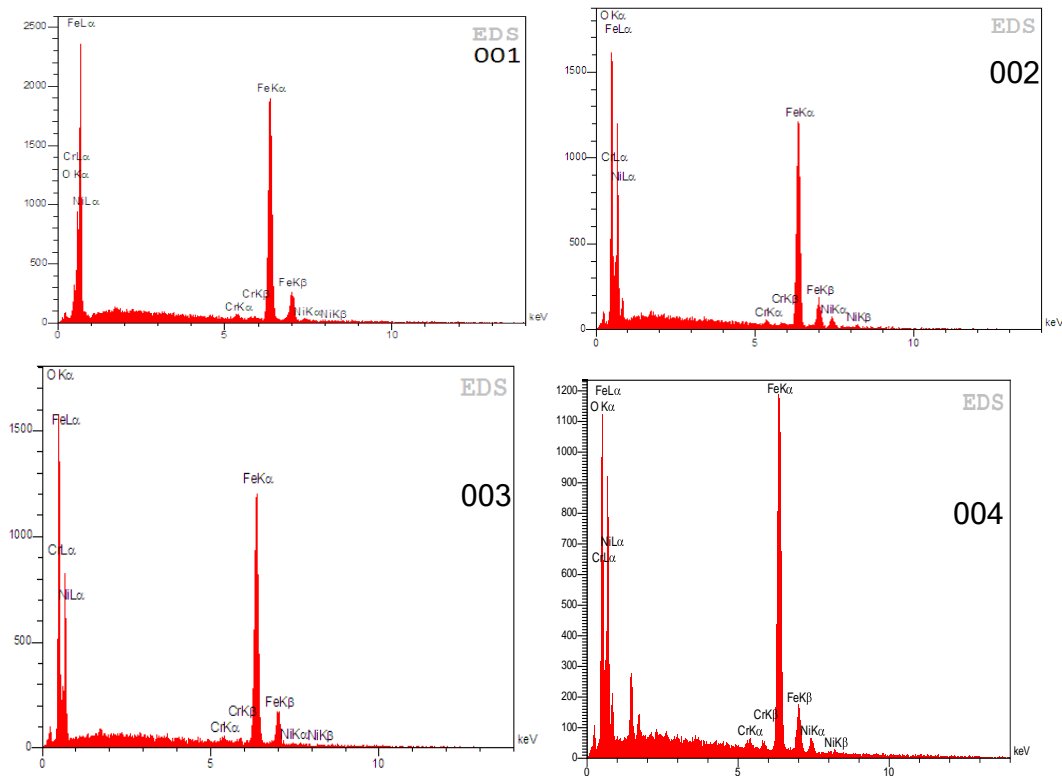
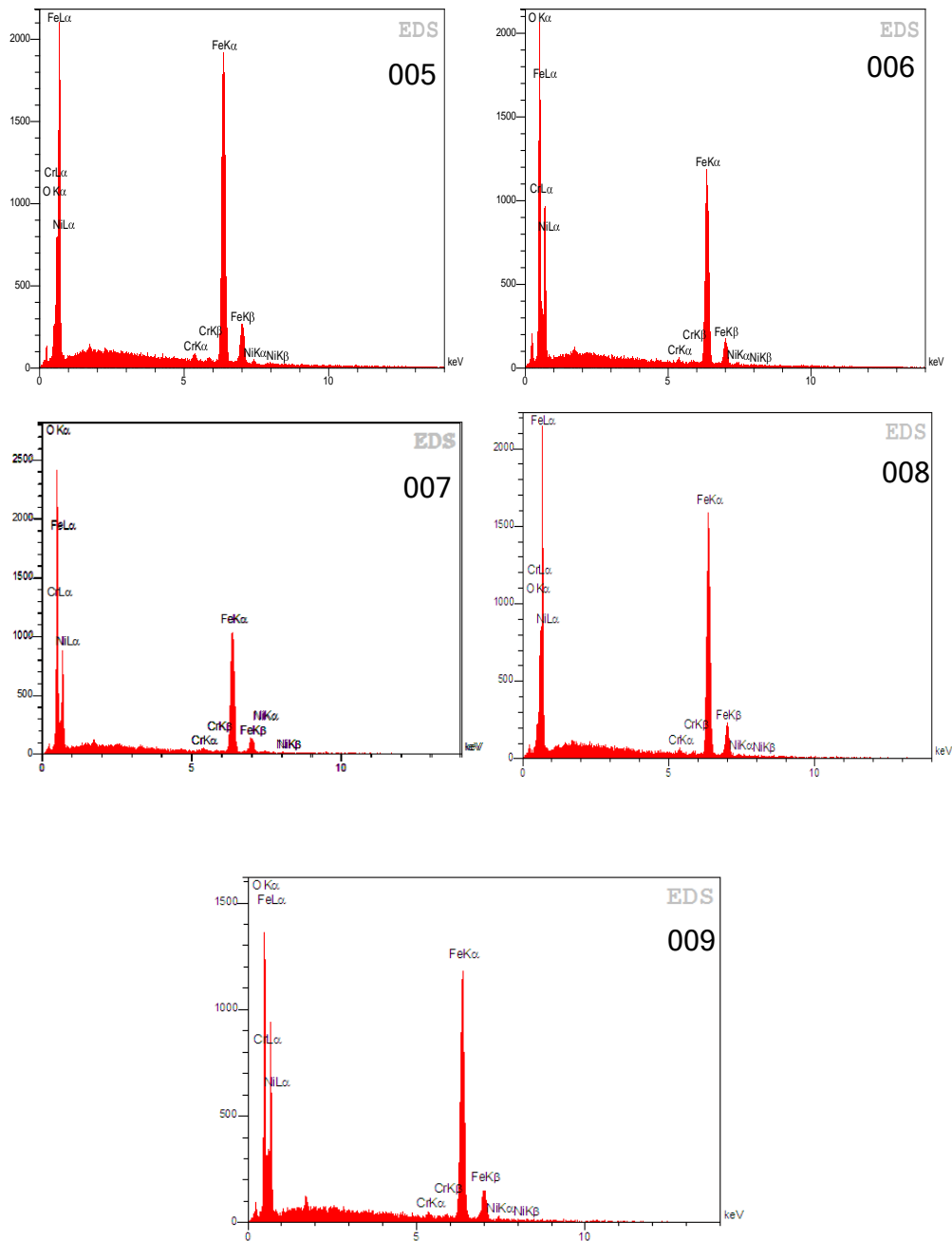


Fig.11. Micrographs FESEM for worn surfaces (a) Nickel-Boron, (b) Nickel-Boron-0.35g/l Carbon nanotube, (c) Nickel-Boron-0.7g/l Carbon nanotube, as-plated; (d) Nickel-Boron, (e) Nickel-Boron-0.35g/l Carbon nanotube, (f) Nickel-Boron-0.7g/l Carbon nanotube as-annealed; (g) Nickel-Boron, (h) Nickel-Boron-0.35g/l Carbon nanotube, (i) Nickel-Boron-0.7g/l Carbon nanotube, plasma nitriding samples.





Figure(12):EDS analysis of worn surface of samples

3.6. Conclusions

Now a day, the characters of plasma nitriding of electroless Ni-B plus (Ni-B-CNT) coating compare with those of annealed one. Under the experimental conditions, coatings of plasma-nitrided of

electroless(Ni-B-CNT) result in the formation of BN and Ni₂B, Ni₃B phases, which increased microhardness of the coatings. Although, the surface roughness increased, but mass loss in plasma nitride coatings decreased to the half of that in the

annealed coating due to the higher microhardness and smoother transition from the case to the core. In conclusion, plasma-nitriding process could be a suitable replacement for annealing procedure to produce more wear resistant electroless coatings investigation. From results that effect of carbon nanotubes experimental on structure of crystallographic of Ni-B electroless during easier of the nucleation of Ni. Increment concentration of CNT source converted from amorphous structure to structure of crystalline. Distribution homogenously of CNT was transformed the morphology of surface coat with filling the crevices and cracks that formed through reaction of the hydrogen evolution. Particle growth and CNT inhibit crystal produce during creation of small nodules but for the sample of (Ni-B-0.7g/l CNT) in which happen the agglomeration because of a large concentration of CNT and so achieve a value higher of surface roughness. When concentration increase of CNT in as-plated samples lead to fall of both specific wear rate and friction coefficient which mainly result from the mechanism of self lubricate of CNT. Whilst for the (Ni-B-0.7g/l CNT), because of their agglomeration and distribution of non-uniform of CNT, produce of increase in coefficient value of the friction. In other hand; plasma-nitrided (Ni-B-CNT) and electroless Ni-B, produce interstitial diffusion of nitrogen atoms in matrix of Ni and creation of Ni₂B, Ni₃B, and BN phases, consequently, increased the hardness. The present of CNT decrement of plastic deformation at the samples of plasma nitriding, as prevented generation of the excessive heat through test of the wear and resistance of the wear was enhanced. The larger resistance of wear related with the sample of (Ni-B-0.35g/l CNT). These can be associated with the smaller size of grain, larger microhardness with distribution of uniform of the CNT. Other work on study

the corrosion resistance properties will be a part of interest

References

1. A. R. Boccaccini and I. Zhitomirsky, *Mater. Sci.*, 6 (2002) 251.
2. D. Thiemig and A. Bund, *Surf. Coat. Tech.*, 202 (2008) 2976.
3. Z. Liu and W. Gao, *Surf. Coat. Tech.*, 200 (2006) 5087.
4. L. p. Wu, J. j. Zhao, Y. p. Xie and Z. d. Yang, *Trans. of Nonferrous Met. Soc. China.*, 2(2010) s630.
5. Riedel A. *Electroless nickel plating*. Finishing Publication LTD., London, 1989.
6. US Patent 2.461.661, 1945.
7. P. Sahoo and S. K. Das, *Mater. Design*, 32 (2011) 1760.
8. Y. Yang, W. Chen, C. Zhou, H. Xu and W. Gao, *App. Nanosci.*, 1 (2011) 19.
9. S. Afroukhteh, C. Dehghanian and M. Emamy, *Mater. Inter.*, 22 (2012) 480.
10. C. Li, Y. Wang and Z. Pan, *Mater. Design*, 47 (2013) 443.
11. V. Vitry, A. Sens, A. F. Kanta and F. Delaunois, *App. Surf. Sci.*, 263 (2012) 640.
12. Y. W. Riddle and T. O. Bailerare, *J. Mater Proc. Tech.*, 57 (2005) 40.
13. T. S. N. Sankara Narayanan, A. Stephan and S. Guruskanthan, *Surf. Coat. Tech.*, 179 (2004) 56.
14. K. Krishnaveni, T. S. N. Sankara Narayanan and S. K. Seshadri, *Surf. Coat. Tech.*, 190 (2005) 115.
15. Z. C. Wang, F. Jia, L. Yu, Z. B. Qi, Y. Tang and G. L. Song, *Surf. Coat. Tech.*, 206(2012) 3676.
16. F. Bülbül, H. Altun, V. Ezirmik and Ö. Küçük, *J. Eng. Tribology.*, (2012) 1-11.
17. T. p. Xuan, L. Zhang and Q. h. Huang, *Trans. Nonfer. Met. Soc. China.*, 16 (2006) 363.
18. H. B. Hassan, Z. A. Hamid, *Int. J. Hydrogen Energy.*, 36 (2011) 849.

19. V. Vitry, A.-F. Kanta, F. Delaunois, Application of nitriding to electroless nickel-boron coatings: chemical and structural effects; mechanical characterization; corrosion resistance, *Mater. Des.* 39 (2012) 269-278 .
20. Y. He, S. Wang, F. Walsh, Y.-L. Chiu, P. Reed, Self-lubricating Ni-P-MoS₂ composite coatings, *Surf. Coat. Technol.* 307 (2016) 926-934.
21. Y. Wan, Y. Yu, L. Cao, M. Zhang, J. Gao, C. Qi, Corrosion and tribological performance of PTFE-coated electroless nickel boron coatings, *Surf. Coat. Technol.* 307 (2016) 316-323.
22. C. Carpenter, P. Shipway, Y. Zhu, Electrodeposition of nickel-carbon nanotube nanocomposite coatings for enhanced wear resistance, *Wear* 271 (2011) 2100-2105.
23. M.-F. Yu, O. Lourie, M.J. Dyer, K. Moloni, T.F. Kelly, R.S. Ruoff, Strength and breaking mechanism of multiwalled carbon nanotubes under tensile load, *Science* 287 (2000) 637-640.
24. P.-C. Tsai, Y.-R. Jeng, J.-T. Lee, I. Stachiv, P. Sittner, Effects of carbon nanotube reinforcement and grain size refinement mechanical properties and wear behaviors of carbon nanotube/copper composites, *Diam. Relat. Mater.* 74 (2017) 197-204.
25. L. Melk, J.J.R. Rovira, M.-L. Antti, M. Anglada, Coefficient of friction and wear resistance of zirconia-MWCNTs composites, *Ceram. Int.* 41 (2015) 459-468.
26. Q. Wang, M. Callisti, A. Miranda, B. McKay, I. Deligkiozi, T.K. Milickovic, A. Zoikis- Karathanasis, K. Hrissagis, L. Magagnin, T. Polcar, Evolution of structural, mechanical and tribological properties of Ni-P/MWCNT coatings as a function of annealing temperature, *Surf. Coat. Technol.* 302 (2016) 195-201.
27. K. Zangeneh-Madar, S. M. MonirVaghefi: *Surf. Coat. Technol.*, 2004, 182, 65–71.
28. Q.-L. Rao, G. Bi, Q.-H. Lu, H.-W. Wang, X.-L. Fan, Microstructure evolution of electroless Ni-B film during its depositing process, *Appl. Surf. Sci.* 240 (2005) 28-33.
29. E. Georgiza, V. Gouda, P. Vassiliou, Production and properties of composite electroless Ni-B-SiC coatings, *Surf. Coat. Technol.* 325 (2017) 46-51.
30. V. Vitry, A.-F. Kanta, F. Delaunois, Application of nitriding to electroless nickel-boron coatings: chemical and structural effects; mechanical characterization; corrosion resistance, *Mater. Des.* 39 (2012) 269-278 .
31. V. Vitry, L. Bonin, Formation and characterization of multilayers borohydride and hypophosphite reduced electroless nickel deposits, *Electrochim. Acta* 243 (2017) 7-17.
32. A. Mukhopadhyay, T.K. Barman, P. Sahoo, Tribological behavior of sodium bor- ohydride reduced electroless nickel alloy coatings at room and elevated temperatures, *Surf. Coat. Technol.* 321 (2017) 464-476.
33. S. K. Das, P. Sahoo: *Tribology in industry.*, 2010, 32, 17-25.
34. M. Anik, E. Korpe, E. Şen, Effect of coating bath composition on the properties of electroless nickel-boron films, *Surf. Coat. Technol.* 202 (2008) 1718-1727.
35. M. HeydarzadehSohi, M. Ebrahimi, A. HonarbakhshRaouf, F. Mahboubi: *Surf.Coat. Technol.*, 2010, 205, S84-S89.
36. G. Prasad Singh, J. Alphonsa, P.K. Barhai, P.A. Rayjada, P.M. Raole, S. ukherjee:*Surf. Coat. Technol.*, 2006, 200, 5807–5811.
37. J. Umeda, B. Fugetsu, E. Nishida, H. Miyaji, K. Kondoh, Friction behavior of network-structured CNT coating on

- pure titanium plate, *Appl. Surf. Sci.* 357 (2015) 721-727
38. M. Yan, H. G. Ying, T. Y. Ma: *Surf. Coat. Technol.*, 2008, 202, 5909–5913.
 39. A. F. Kanta, V. Vitry, F. Delaunois: *Mater. Lett.*, 2009, 63, 2662–2665.
 40. V. Vitry, A.-F. Kanta, F. Delaunois, Mechanical and wear characterization of electroless nickel-boron coatings, *Surf. Coat. Technol.* 206 (2011) 1879-1885.
 41. L.Y. Wang, J. Tu, W. Chen, Y. Wang, X. Liu, C. Olk, D. Cheng, X. Zhang, Friction and wear behavior of electroless Ni-based CNT composite coatings, *Wear* 254 (2003) 1289-1293
 42. V. Puchy, P. Hvizdos, J. Dusza, F. Kovac, F. Inam, M. Reece, Wear resistance of Al₂O₃-CNT ceramic nanocomposites at room and high temperatures, *Ceram. Int.* 39 (2013) 5821-5826.
 43. K. Krishnaveni, T. S. N. Sankara Narayanan, S. K. Seshadri: *Surf. Coat. Technol.*, 2005, 190, 115–121.
 44. M. Palaniappa, S. K. Seshadri: *Wear.*, 2008, 265, 735–740.
 45. M.M. Bastwros, A.M. Esawi, A. Wifi, Friction and wear behavior of Al-CNT composites, *Wear* 307 (2013) 164-173.
 46. I.-Y. Kim, J.-H. Lee, G.-S. Lee, S.-H. Baik, Y.-J. Kim, Y.-Z. Lee, Friction and wear characteristics of the carbon nanotube-aluminum composites with different manufacturing conditions, *Wear* 267 (2009) 593-598.